



Molecular Identification of Spatially Distinct Anabolic Responses to Mechanical Loading in Murine Cortical Bone

Carolyn Chlebek, 1 D Jacob A Moore, 2 F Patrick Ross, 3 and Marjolein C H van der Meulen 1,4 D

ABSTRACT

Osteoporosis affects over 200 million women worldwide, one-third of whom are predicted to suffer from an osteoporotic fracture in their lifetime. The most promising anabolic drugs involve administration of expensive antibodies. Because mechanical loading stimulates bone formation, our current data, using a mouse model, replicates the anabolic effects of loading in humans and may identify novel pathways amenable to oral treatment. Murine tibial compression produces axially varying deformations along the cortical bone, inducing highest strains at the mid-diaphysis and lowest at the metaphyseal shell. To test the hypothesis that load-induced transcriptomic responses at different axial locations of cortical bone would vary as a function of strain magnitude, we loaded the left tibias of 10-week-old female C57BI/6 mice in vivo in compression, with contralateral limbs as controls. Animals were euthanized at 1, 3, or 24 hours post-loading or loaded for 1 week (n = 4-5/group). Bone marrow and cancellous bone were removed, cortical bone was segmented into the metaphyseal shell, proximal diaphysis, and mid-diaphysis, and load-induced differential gene expression and enriched biological processes were examined for the three segments. At each time point, the mid-diaphysis (highest strain) had the greatest transcriptomic response. Similarly, biological processes regulating bone formation and turnover increased earlier and to the greatest extent at the mid-diaphysis. Higher strain induced greater levels of osteoblast and osteocyte genes, whereas expression was lower in osteoclasts. Among the top differentially expressed genes at 24-hours post-loading, 17 had known functions in bone biology, of which 12 were present only in osteoblasts, 3 exclusively in osteoclasts, and 2 were present in both cell types. Based on these results, we conclude that murine tibial loading induces spatially unique transcriptomic responses correlating with strain magnitude in cortical bone. © 2022 American Society for Bone and Mineral Research (ASBMR).

KEY WORDS: BIOMECHANICS; MOLECULAR PATHWAYS—REMODELING; CELL/TISSUE SIGNALING—TRANSCRIPTION FACTORS; OSTEOPOROSIS; PRECLINICAL STUDIES

Introduction

steoporosis is a disease resulting in decreased bone mass and mineralization, often leading to increased fracture risk. In the United States, osteoporosis affects 7 to 12 million people. The majority of osteoporosis treatments target osteoclasts by administering one of a family of bisphosphonates, which reduce bone resorption, but fail to increase bone formation. In contrast, anabolic treatments reduce fracture risk by increasing bone mass, are unsatisfactory for long-term use because the initial increase in bone formation is followed by increased resorption, limiting anabolic effects to a period known as the anabolic

window. (2,6,7) Therefore, enhanced understanding of anabolic models may facilitate identification of new mechanisms involved in bone formation.

Mechanical loading of the skeleton produces anabolic tissue responses and increases bone mass. (8) In premenopausal women, targeted resistance and high-magnitude loading exercises increase bone mineral density at the hip, (9,10) lumbar spine (9,10) and radius. (11) In vivo rodent models provide a controlled setting to examine the mechanisms underlying the anabolic effects of mechanical loading. (12) Cyclic compressive loading of the murine tibia in young female mice stimulates bone growth. (13,14) This anabolic tissue response is driven by a cascade of osteogenic signaling pathways, few of which have been identified in the context of in vivo tibial

Received in original form February 19, 2022; revised form August 5, 2022; accepted August 20, 2022.

Address correspondence to: Marjolein C H van der Meulen, PhD, Meinig School of Biomedical Engineering, Cornell University, 121D Weill Hall, Ithaca, NY 14853, USA. E-mail: mcv3@cornell.edu

Additional Supporting Information may be found in the online version of this article.

Journal of Bone and Mineral Research, Vol. 37, No. 11, November 2022, pp 2277–2287. DOI: 10.1002/jbmr.4686

© 2022 American Society for Bone and Mineral Research (ASBMR).

¹Meinig School of Biomedical Engineering, Cornell University, Ithaca, NY, USA

²College of Agriculture and Life Sciences, Cornell University, Ithaca, NY, USA

³FPR Scientific Consulting, Amherst, MA, USA

⁴Hospital for Special Surgery, New York, NY, USA

loading,⁽¹⁵⁾ suggesting that more may remain to be discovered.

RNA sequencing is an unbiased analysis that can identify the transcriptomic responses driving load-induced bone formation. Gene expression profiles may provide insight into the biological pathways driving the osteogenic response initiated by in vivo loading. The transcriptomic response of bone to loading shifts from increased gene expression for energy metabolism at early time points. (16) to increased osteogenic gene expression at later time points. In addition to temporal transcriptomic differences, tissue-specific differences are evident in the tibia, with the metaphyseal cortical and cancellous bone each having unique transcriptional profiles following loading. (18)

Because of the curvature of the murine tibia, compressive loading induces bending and axially varying strains along the cortex (Fig. 1A, B). (19) Based on finite element model predictions, the magnitude of the principal strains increases axially along the tibial cortex, from 1000 μE at the metaphyseal cortical shell to 1500 μE at the proximal diaphysis and 2000 μE at the mid-diaphysis. (20) The greatest tensile strains occur at the periosteal surface at the diaphysis and endocortical surface in the metaphysis. (21) Anabolic pathways in cortical bone that are differentially activated based on strain magnitude may identify promising novel therapeutic targets and have not been explored in previous transcriptomic studies. We hypothesized that the transcriptional profile of tibial cortical bone under compression would vary both

with time and as a function of the strain magnitude within the tissue, reflected by the axial tissue location. Therefore, we applied compressive loading to the mouse tibia, segmented the cortical bone based on strain magnitude, and examined the transcriptional responses at both early and late time points.

Materials and Methods

Mice

Female 10-week-old female C57Bl/6J mice (Jackson Laboratory, Bar Harbor, ME, USA) were subjected to in vivo mechanical loading of the left tibia under general anesthesia (2% isoflurane, 1.0 L/min, Webster) in this IACUC-approved study. The knee was held fixed, and load was applied by an actuator located at the bottom of the foot (Fig. 1C). Triangular loading waveforms with a 9 N peak load were applied at 4 Hz for 1200 cycles per day (Fig. 1D). Mice resumed normal cage activity outside of the loading sessions and were housed 3 to 6 per cage. Animals had free access to chow (Teklad LM-485, Envigo 7912, Indianapolis, IN, USA).

Time points were selected to capture both early and long-term transcriptional responses to tibial loading. To examine early time points, mice were euthanized by cervical dislocation at 1 hour (n = 5), 3 hours (n = 4), or 24 hours (n = 4) after the completion of loading (Fig. 1*E*). To evaluate long-term time points,

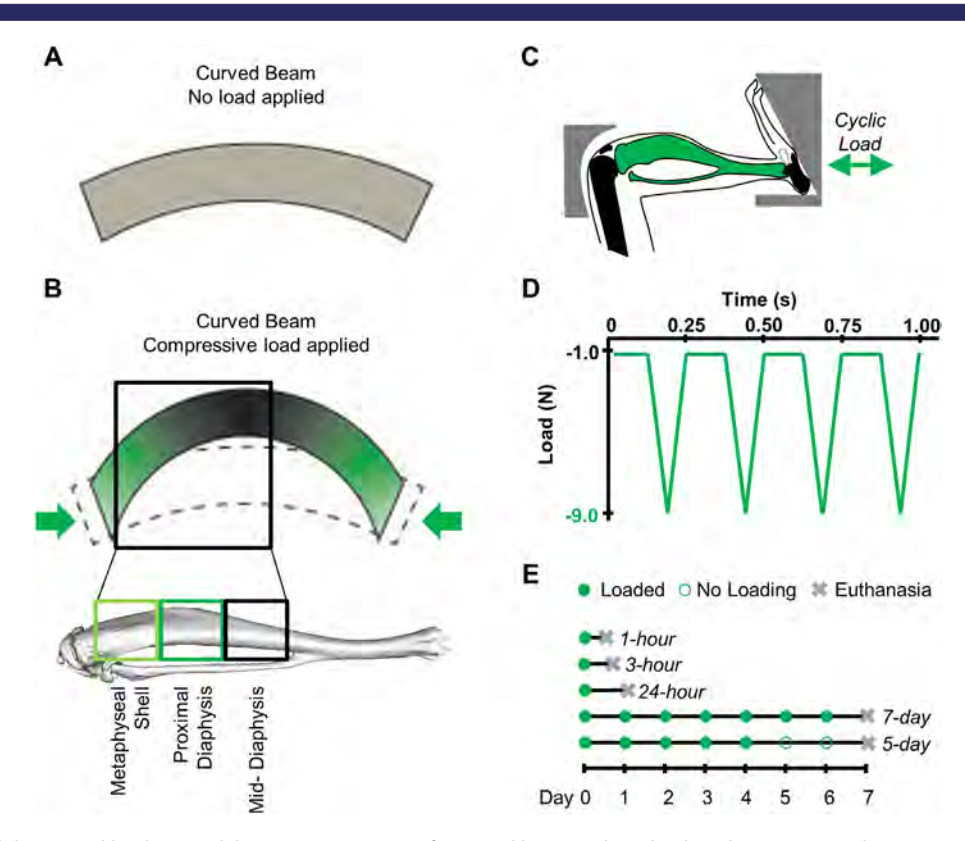


Fig. 1. Experimental design and loading model. (A) Representation of a curved beam without load application. (B) Under compressive loading, a curved beam experiences maximum strains at the center. Compression of the mouse tibia is analogous to a curved beam with peak strains at the mid-diaphysis and a decreasing strain gradient along the proximal cortex. (C) Schematic of non-invasive mouse tibial loading configuration. Knee and ankle were held, and compression was applied across the entire lower limb. (D) Cyclic loading waveform for loading at 9 N-peak magnitude. (E) Summary of time-dependent studies. Ten-week-old C57Bl/6 female mice underwent one or more bouts of tibial loading. To examine short-term transcriptomic responses, mice were euthanized at 1 hour, 3 hours, or 24 hours after loading. To measure later transcriptomic responses, two groups of mice were euthanized after 7 days of daily loading, and the second after 5 days of loading and 2 days of rest. n = 4-5/group.

mice received daily cyclic compressive loading for 7 consecutive days (n = 4) and were euthanized 24 hours after the last loading bout. Previous long-term loading studies defined 1 week as 5 consecutive days of loading, followed by 2 rest days. (13,14,22,23) To evaluate potential differences induced by this rest period, a final group received 5 consecutive days of loading with euthanasia on the eighth day after the first loading session (n = 5). Both tibiae were dissected, and soft tissue removed. Bone marrow was removed through centrifugation, and cancellous bone was removed from the metaphysis. (24) Finally, the cortical bone was segmented into three sections: metaphyseal cortex, proximal diaphysis, and middiaphysis, resulting in six samples per mouse (Fig. 1B).

RNA sequencing

All tissues were flash-frozen in liquid nitrogen. Trizol was added for pulverization (Life Technologies, Carlsbad, CA, USA). All methods were performed with sterile reagents under sterile conditions in a randomized, blinded fashion. Samples were pulverized (Sartorius Mikro-dismembrator S, Sartorius Stedim Biotech, Bohemia, NY, USA) for 5 minutes at 2600 rpm in tubes containing 2.8-mm ceramic beads. RNA was isolated using a phenol-chloroform extraction (Qiagen RNeasy kit, Qiagen, Germantown, MD, USA; with DNase digest). (24) All samples had an RNA Quality Number ≥6.0 (3730xl DNA Analyzer, Applied Biosystems, Waltham, MA, USA). 3' RNA sequencing was performed (NextSeg500, Illumina, San Diego, CA, USA), (25) which produces a single sequence per transcript to limit expression bias from longer transcripts.

Transcripts were aligned to the mm10 genome (STAR⁽²⁶⁾). Samples had an average of 3.4 million reads, and 74% of reads were mapped uniquely to the mouse genome. Each sample contained over 1 million reads. Genes with less than 3 counts per million were not included for analysis. Differential expression between loaded and control limbs was determined using a paired design (edgeR⁽²⁷⁾) and defined as genes with a fold-change >2 or <-2 with a <0.05 false discovery rate (FDR). To examine biological processes, genes with HUGO references and their associated fold changes were imported into Gene Set Enrichment Pre-Ranked Analysis, with FDR < 0.25 considered for examination. (28) Established pathway databases (GO, (29,30) Reactome, (31) GSEA Hallmark⁽²⁸⁾) were included.

Bulk RNA-sequencing does not provide evidence for quantitative assessment of cell populations, yet examination of individual genes can give insight into the transcriptional activity level of specific cell types. Thus, we used Runx2, (32) Bglap, (33) and Col1a1^(34,35) as a measure of transcriptional activity associated with osteoblasts. Osteocyte-associated genes were separated by mineralizing osteocytes (Dstn [Destrin], (36) Phex, (37) and $Dmp1^{(38)}$) and mature osteocytes ($Sost^{(39)}$ and $Mepe^{(40)}$). $Acp5^{(41)}$ and Ctsk⁽⁴²⁾ were used to assess osteoclast activity. To examine these individual genes, we compared normalized gene counts (reads per million mapped reads calculated in DESeg2 with Trimmed Mean of M values correction (43) across all groups using a linear mixed-effects model with factors of loading, time point, and tissue segment (p < 0.05) (random effect: mouse). All results presented are significant unless stated.

mRNA in situ hybridization

mRNA expression of Ctsk and Sost was validated at 24 hours after loading using in situ hybridization (n = 5). After

euthanasia, whole tibiae were fixed in neutral buffered formalin and decalcified in 10% EDTA. Limbs then were embedded in paraffin and sectioned at 6-µm thickness from medial to lateral. RNAscope© 2.5 HD Duplex kit (ACD, Newark, CA, USA) with ACD custom bone reagent was applied with Sost and Ctsk probes to visualize the gene expression. Images were obtained with a brightfield slide scanner (Aperio Scanscope, Leica Biosystems, Danvers, MA, USA), and all cortical regions examined. Individual Sost transcripts were quantified (HALO Image Analysis Platform, Indica Labs, Albuquerque, NM, USA). The multinucleation and high expression levels of Ctsk precluded assessment of individual probes in osteoclasts. Therefore, areas of positive (blue) and strong positive (dark blue) pixels correlating to Ctsk probes were quantified (Fig. 5E; Aperio ImageScope, Leica Biosystems). Linear mixed-effects models with factors of loading and tissue segment (p < 0.05) were used to validate differences in both Sost and Ctsk transcripts (random effect: mouse). Negative controls were used to demonstrate little to no signal (1 dot or less per 10 cells, RNAscope guidelines). Visualization of positive control probes for (1) Gapdh, a commonly used control gene, and (2) Polyubiquitin-C (Ppib), a control gene recommended for RNAscope©, demonstrated appropriate RNA quality and optimal permeabilization (Supplemental Fig. S6).

Results

High-strain cortical segment (mid-diaphysis) had greatest number of load-induced differentially expressed genes

The number of differentially expressed genes (DEG) varied in each cortical segment, paralleling the magnitude of strain induced by loading. Across all time points, the mid-diaphysis consistently had the most DEG with loading, whereas the metaphyseal cortical shell had the least, with an intermediate value at the proximal diaphysis (Fig. 2A; Supplemental Figs. S1 and S2A-C). When all tissue segments were combined for a given time point, the greatest number of DEG were present later. Among the early time points, 3 hours post-loading had the greatest number of DEG across all three cortical segments. At the mid-diaphysis, a high proportion of genes was downregulated early compared with later time points (1 hour: 63%; 3 hours: 65%; 24 hours: 61%; 5 days: 36%; 7 days: 46%).

With loading, DEG included a small number of genes important for bone biology. In contrast, the majority of genes either did not code for proteins or their transcribed products had no demonstrable function in bone. Thus, of the top 170 DEG at 24 hours, only 17 had established roles in bone cells with the majority related to osteoblast activity (n = 14), with fewer linked to osteoclasts (n = 5) (Supplemental Fig. S2D). The major DEG whose products are contributors to bone formation and osteoblast function included transcription factors (Gli1, (44) Satb2, (45) Sox8, (46) Foxp1(47), enzymes (Chka, (48) Lox, (49) Cdo1(50), and matrix-related genes (Vcan, (51) Gorab, (52) Kdelr2(53)). Osteoblastrelated genes Npy and Axin2 were upregulated with loading and respectively encode a neuropeptide that binds to its receptor on osteoblasts to enhance their function⁽⁵⁴⁾ and a regulator of Wnt signaling, a major osteogenic pathway.⁽⁵⁵⁾ Two osteoclastrelated genes linked to resorption, Fam98a⁽⁵⁶⁾ and Traf6, (57)</sup> were also upregulated with loading, whereas Ttpa, (58) a gene whose product attenuates osteoclastogenesis, was downregulated. The skeletal roles of two upregulated genes, Cgref1⁽⁵⁹⁾ and

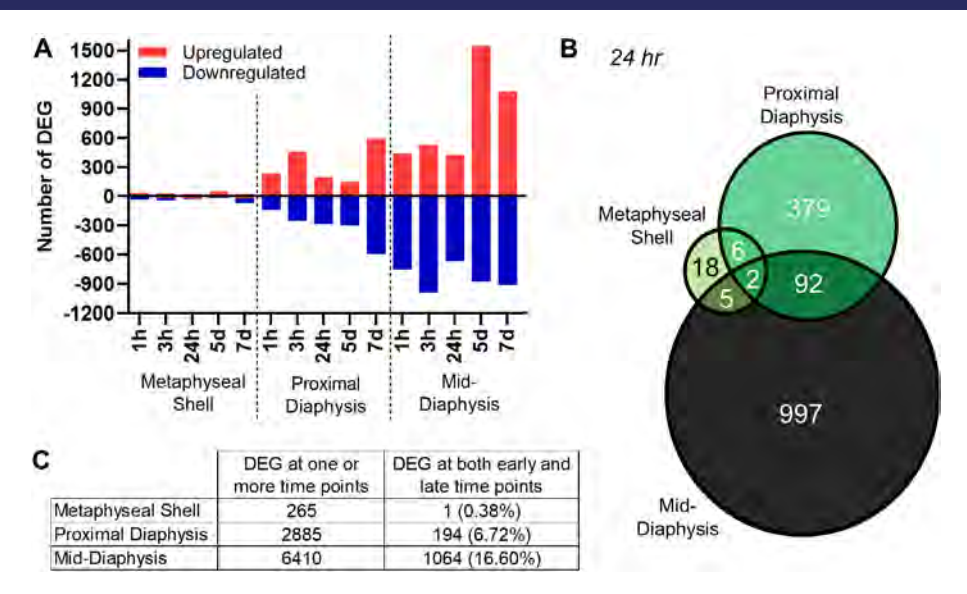


Fig. 2. The three cortical regions exhibited variable transcriptional response to loading, with the greatest response at the mid-diaphysis. (*A*) The total number of differentially expressed genes (DEG) altered with loading at each time point across tissue segments. (*B*) The majority of DEG were unique to each tissue segment and not shared, as shown in the 24-hour Venn diagram. Similar results were obtained at the other time points (Supplemental Fig. S3). (*C*) Number of DEG shared between early and late time points.

Cthrc1,^(60,61) are uncertain because both have been reported in osteoblasts and osteoclasts.

At each time point, the three cortical segments shared few DEG induced by loading (Fig. 2B and Supplemental Fig. S3). The greatest proportion of genes were shared consistently between the proximal and mid-diaphysis. The adjacent metaphyseal shell and proximal diaphyseal segment shared a similar fraction of genes as the non-adjacent metaphyseal shell and mid-diaphysis. Only four genes with established roles in bone, Fosb, (62) Tnfrsf11b, (63) Anpep, (64) and Col3a1, (65,66) were shared across all three segments.

One week of loading resulted in greater transcriptomic response than early time points

Within each tissue segment, few DEG were shared across time points (Fig. 2C). At early time points, transcriptomic changes with loading were distinct; only 23 DEG in the mid-diaphysis were shared among 1, 3, and 24 hours post-loading. The later time points induced different transcriptomic responses than the early time points, with few DEG shared between early and late time points (Fig. 2C). Additionally, gene expression assessed 24 hours after the last loading bout (7 days) was different when compared

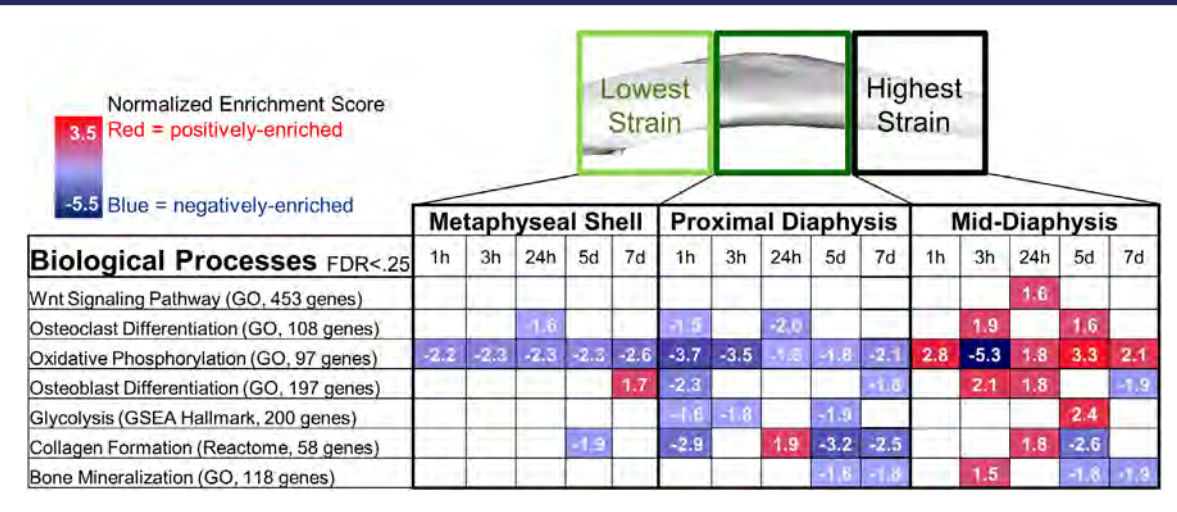


Fig. 3. Detailed pathway analysis of cortical bone tissue responses to loading (enrichment score with loading relative to control). Numerous pathways were positively enriched at the mid-diaphysis, but few were increased at the metaphyseal shell. Processes regulating bone formation and turnover were initiated earlier in the segment of highest strain (mid-diaphysis) and later in lower strain segments (metaphyseal shell).

with findings after the last loading bout (5 days) with only 17% of the DEG at the mid-diaphysis shared. Between 5 and 7 days of loading, transcriptomic changes continued.

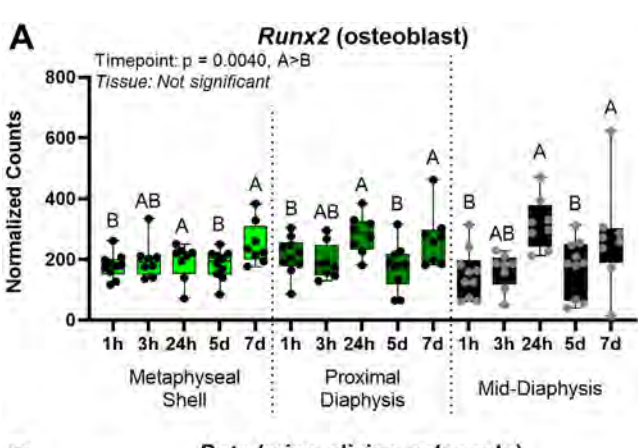
Higher strain correlated with earlier and greater activation of bone formation pathways

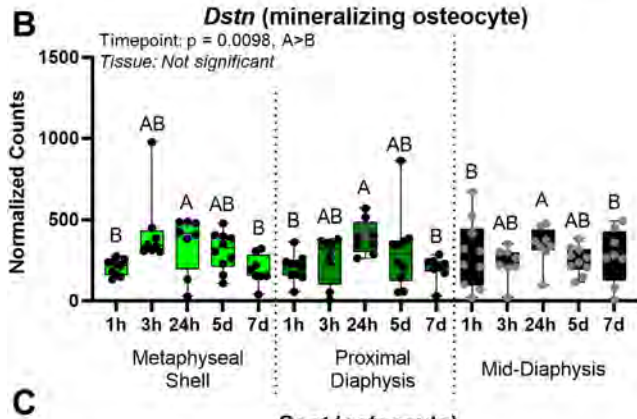
When biological pathways associated with load-induced bone formation were considered, the mid-diaphysis had the earliest and largest positive enrichment with loading (Fig. 3). Oxidative phosphorylation was the first pathway enriched at the middiaphysis and remained elevated across all but one time point. In contrast, the metaphyseal shell and proximal diaphysis had mostly negative enrichment of processes related to bone formation and/or development, with the exception of positive enrichment of differentiation of osteoblasts and osteoclasts and bone mineralization at 3 hours. The Wnt signaling pathway, previously associated with loading, was enriched only at the mid-diaphysis at 24 hours. Further investigation of genes within the Wnt signaling pathway (GO) revealed that the greatest load-induced fold changes were at the mid-diaphysis and the smallest at the metaphyseal shell (Supplemental Fig. S4). Despite both the metaphyseal shell and proximal diaphysis having few positively enriched processes related to bone formation, the pathways activated were different temporally and functionally. Mice subjected to multiple loading doses had larger numbers of negatively enriched pathways, suggesting that the activation had ceased.

Several pathways that were highly enriched with loading had not been associated with bone formation previously. One clear example involved muscle processes such as Muscle Contraction, Contractile Fiber, Actin Myosin Filament Sliding (all GO terms). Positive enrichment of muscle processes occurred first in the mid-diaphysis (1 hour) and later in the proximal diaphysis and metaphyseal cortical shell (3 hours). Reinforcing the tissuespecific and time-dependent nature of our findings, the middiaphysis had the earliest negative enrichment of muscle-related biological processes, starting at 3 hours, whereas the proximal diaphysis and metaphyseal cortical shell had negative enrichment only after 5 days. The muscle processes followed the same strain-driven pattern of the known bone anabolic pathways. DEG with loading that are traditionally functional in muscle, including Pamr1, Myh2, and Myl2, were likely driving the enrichment of these muscle processes.

Bone cell activity varied temporally and spatially across the cortical segments

Levels of genes uniquely expressed in osteoblasts, osteocytes, and osteoclasts were examined to determine shifts in activity of these cell types with loading. Major genes associated with osteoblast-lineage cells, namely Runx2, Bglap, 33 and Col1a1, 43,35 varied temporally across the experiment but not spatially along the cortex (Fig. 4A). Although the effect of loading was not significant, the normalized counts of osteoblast-related genes were most elevated 24 hours and 7 days post-loading. Genes that mark mineralizing osteocyte activity (Dstn [Destrin], 9hex, 37 and Dmp1 limbs (Fig. 4B). Similar to osteoblast activity, higher normalized counts for Dstn, a gene expressed by mineralizing osteocytes, were measured 24 hours post-loading compared with 1-hour and 7-day time points.





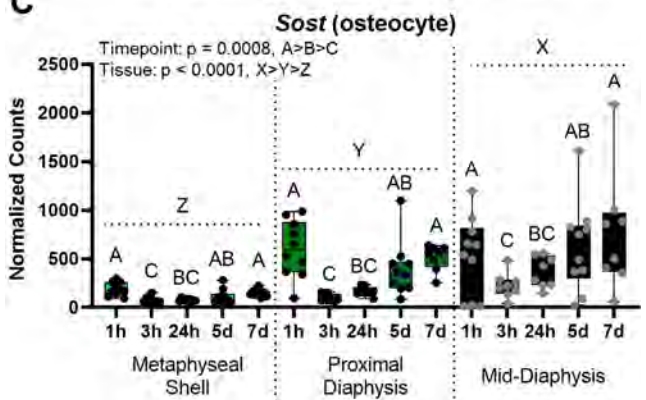


Fig. 4. Normalized counts of genes associated with osteoblasts (Runx2), mineralizing osteocytes (Dstn), or mature osteocytes (Sost). Gene expression was used to estimate changes in cell population or activity with time across the three cortical segments. The p values are shown for 3-way ANOVA to evaluate effects of Time point, Tissue segment, and Load. The effect of Loading was not significant, and loaded and control limbs were combined. Significant effects (p < 0.05) indicated by letters: A > B > C for Time point differences, X > Y > Z for Tissue segment differences. (A) Normalized gene counts for Runx2, a marker of osteoblasts, were greatest at 24 hours and 7 days post-loading. (B) Normalized gene counts for Dstn, reflecting mineralizing osteocytes, were significantly increased 24 hours post-loading. (C) Mature osteocyte activity may be altered both with time and across tissue segments. Normalized gene counts of Sost were lowest at 3 and 24 hours post-loading. Spatially, the mid-diaphysis had the greatest Sost activity, followed by the proximal diaphysis and metaphyseal shell.

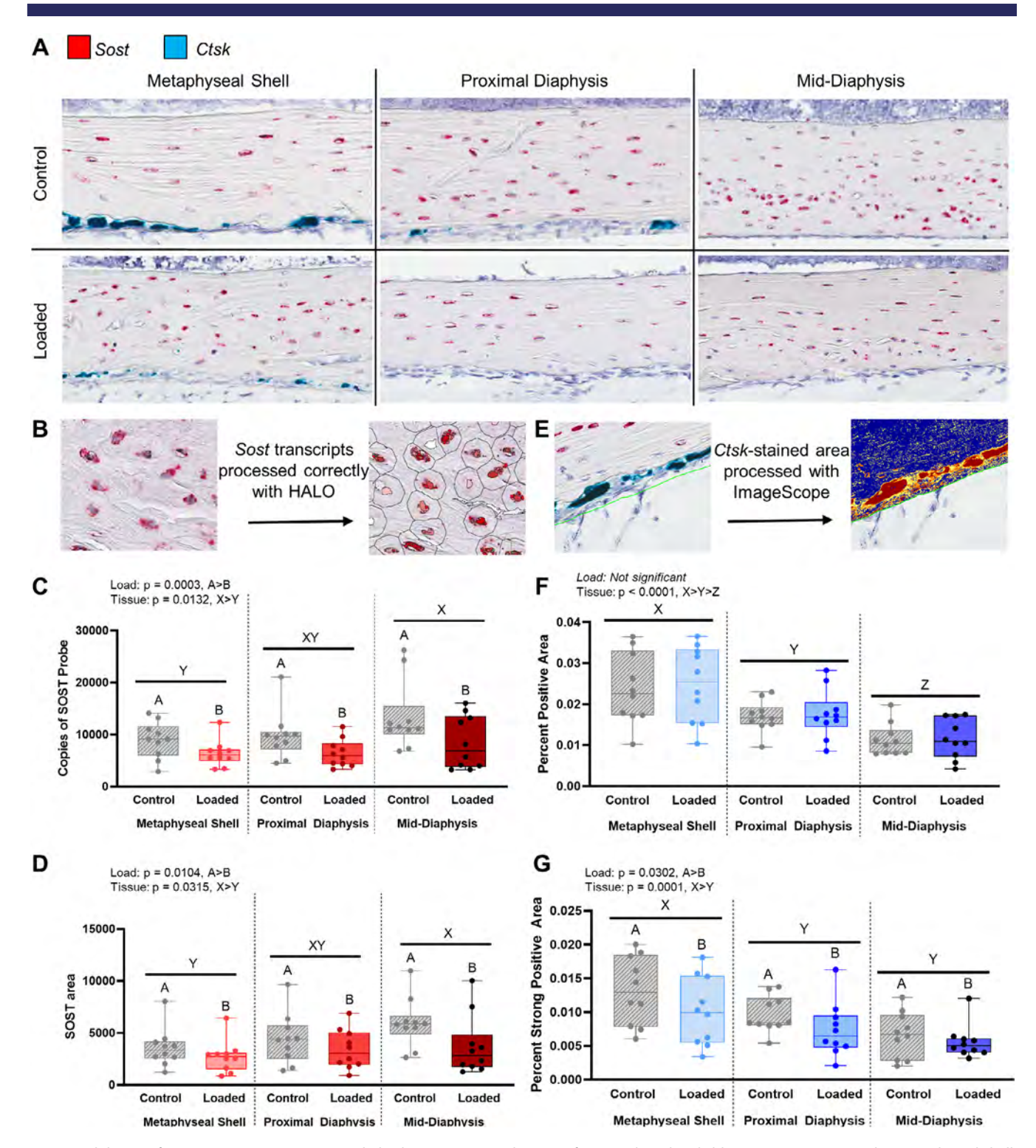


Fig. 5. Validation of gene expression using in situ hybridization. (*A*) Visualization of Sost (red) and Ctsk (blue) expression across the metaphyseal shell, proximal diaphysis, and mid-diaphysis of control and loaded limbs. (*B*) To quantify Sost, HALO software was used to identify the number of probes and cells. (*C*, *D*) Sost probes and area were decreased with loading, and varied by cortical location. (*E*) To quantify Ctsk, pixels were classified as strong positive (red area) or positive (orange area). Loading decreased Ctsk percent area both moderately (*F*) and strongly (*G*). For both Sost and Ctsk quantification, *p* values are shown for 2-way ANOVA to evaluate the effects of Tissue segment and Load. Significant effects (p < 0.05) displayed by letters: A > B for load differences, X > Y > Z for tissue differences.

Mepe⁽⁴⁰⁾ and Sost⁽³⁹⁾ expression were used to evaluate mature osteocytes. Sost expression was greater at 1 hour and 7 days (Fig. 4C).

Gene expression identifying mature osteocytes and osteoclasts varied with cortical tissue location. The mid-diaphysis (highest strain) had significantly greater levels of Sost and Mepe, whereas the metaphyseal shell (lowest strain) had the lowest levels (Fig. 4C). Conversely, expression of osteoclast genes, Acp5⁽⁴¹⁾ and Ctsk,⁽⁴²⁾ was greatest in the metaphyseal shell and lowest in the mid-diaphysis (Supplemental Fig. S5), Levels of Sost and Ctsk reflected the degree of strain at each cortical segment, with expression changing progressively from the metaphyseal shell to the mid-diaphysis (Fig. 4C and Supplemental Fig. S5). Sost and Ctsk gradients were inverse, reflecting a bias toward increased bone formation in the mid-diaphysis compared with the metaphyseal shell.

Sost and Ctsk expression decreased with loading and were present in unique cell populations

To validate the sequencing data, we examined in situ hybridization of Sost and Ctsk, definitive markers for osteocytes and osteoclasts, using RNAscope©, HALO, and ImageScope technology (Fig. 5). We selected these two DEG because at 24 hours postloading, Sost was downregulated at the mid-diaphysis (fold change [FC] = -2.34) and Ctsk was downregulated at the metaphyseal shell (FC = -2.29) and proximal diaphysis (FC = -2.38). For in situ hybridization, an additional group of mice were euthanized 24 hours after a single loading bout (n = 5), and Sost and Ctsk transcripts identified in sagittal sections. As expected, Sost transcripts were expressed by embedded bone cells, whereas Ctsk was expressed by bone-lining cells (Fig. 5A). With in situ hybridization, Sost and Ctsk expression were lower in loaded limbs compared with control limbs (Fig. 5C, D, F, G). Sost expression was greater at the mid-diaphysis compared with the metaphyseal shell. Conversely, Ctsk expression was lowest at the mid-diaphysis, for both areas containing positive and strong positive pixels.

Discussion

Understanding the anabolic mechanisms that stimulate bone formation after mechanical loading may yield insights into potential therapeutic targets to treat osteoporosis. In the present study, we demonstrated that the transcriptomic response of cortical bone to loading varied as a function of cortical location, correlating with strain magnitude. Gene expression in each cortical tissue segment was distinct, with few genes shared among segments. Additionally, most DEG were novel and have no established functions within bone. Of the genes with recognized functions in bone, the majority were associated with anabolic bone formation rather than catabolism. Anabolic responses to loading were initiated first at the segment of highest strain (mid-diaphysis) and later at the lowest strain segment (metaphyseal shell), reflecting the axial strain gradient along the tibia. The changes we observed in differentially expressed genes, enriched biological processes, and cell-specific gene expression all suggest strain gradient-induced differences along the cortex.

The transcriptomic responses of the cortical segments likely were driven by the load-induced strain within the tissues rather than by the tissue location. The lack of shared DEG between tissue segments indicates a unique response within each bone segment, highlighting the localized nature of the transcriptomics. These local responses would not have been apparent in an analysis of the entire cortical diaphysis or whole bone. Bending induced by compression of the curved tibia produces higher strain levels at the diaphyseal segments compared with the metaphyseal cortical shell (Fig. 1B), which primarily undergoes compression. (19) The area of neutral strain in transverse sections of the tibia decreases distally along the cortex, with finite element models confirming increased mean principal strains and frequency of maximal tensile and compressive strains at the mid-diaphysis compared with the metaphyseal cortical shell. (21,67) Furthermore, the metaphyseal cortical shell is the only cortical segment that shares load with cancellous bone, resulting in the lowest tissue strains, which correlated with a smaller and later transcriptomic response to loading.

At a molecular level at 24 hours post-loading, we found changes in the levels of 17 of the top DEG whose products modulate bone formation and/or resorption. Most of these genes were upregulated with loading and have well-established functions related to osteoblasts, consistent with the net anabolic response of in vivo loading. However, two genes (Cgref1 and Cthrc1) were reported in both osteoblasts and osteoclasts (Supplemental Fig. S2), and thus their overall role in the response to loading is unclear. Cgref1 suppresses AP-1 signaling, which is downstream of agonistic receptors in both osteoblasts and osteoclasts. (59) Targeted deletion of the gene in each cell type is needed to identify the dominant target cell. The function of CTHRC1is more complex. The secreted protein was first reported to play a role in osteoblast proliferation and differentiation, (68) yet targeted deletion in osteoblasts did not affect bone mass. (69) In contrast, mice lacking Cthrc1 in osteoclasts were osteopenic due to reduced bone formation, confirming that CTHRC1 is an osteoclast-derived coupling factor. (69) Deletion of Tpbq, (60) which codes for a CTHRC1 receptor on osteoblasts, and PHLPP1, (61) which enhances Cthrc1 expression in osteoclasts, provided convincing evidence that CTHRC1 is a coupling factor impacting both osteoblasts and osteoclasts. Once again, tissue-specific gene deletion will yield additional insights.

Examining the enrichment of biological processes allowed us to integrate the differential expression of individual genes. Biological processes associated with bone formation were enriched earlier, and to a greater extent, at the highest strain segment and later at the lowest strain segment. After the initiation of bone remodeling via mechanoresponsive pathways, (70) new bone cells likely were recruited through the differentiation of osteoclasts and osteoblasts, which rely on oxidative phosphorylation⁽⁷¹⁾ and glycolysis, ⁽⁷²⁾ respectively. Oxidative phosphorylation was enriched significantly across all time points and tissues examined, in agreement with previous loading studies. (16,73) The negative enrichment of osteoclast differentiation and oxidative phosphorylation in the metaphyseal shell and proximal diaphysis implies less osteoclast differentiation, eventually resulting in fewer bone-resorbing cells, consistent with the anabolic effect of loading. The final stages of bone remodeling involve collagen formation and bone mineralization. Surprisingly, these processes were negatively enriched after 1 week of loading, perhaps indicating the transcriptomic response concluded at an intermediate time point not included here.

The differential expression and pathway enrichment associated with muscle tissue in our data set corroborates findings from previous studies that muscle-associated genes were differentially expressed in bone tissue with loading, despite the absence of muscle in the bone samples. (18) Muscle and bone

are related mechanically and both undergo exercise-induced growth and disuse-related reductions in size and quality. Biochemical tissue cross-talk occurs via factors secreted by bone cells affecting muscle and muscle-derived factors that influence bone. Finally, multiple genes are shared between traditional muscle-related pathways and oxidative phosphorylation. Therefore, the activity of muscle-related genes and biological processes after mechanical loading of bone was not surprising.

Including both early and late time points in this study provided a timeline of the skeletal transcriptomic response to loading. Cell-specific gene expression reflects cellular responses to loading likely through a combination of activity early and proliferation later. The life span of osteoclasts and osteoblasts is typically on the order of days to weeks⁽⁷⁵⁾; therefore, the increased expression of genes associated with these cells over the period under examination probably implicates cell activity rather than a shift in cell number. Systemic increased levels of Runx2 and Dstn at 24 hours after loading suggest increased activity of osteoblasts⁽³²⁾ and mineralizing osteocytes⁽³⁶⁾ early in the response to loading. At 7 days, more osteoblasts may be present, and thus the increased expression level of Runx2 may reflect an increase in their numbers, a point that warrants further investigation. Altered gene expression associated with mature osteocytes after 1 week suggests their involvement in sensing and responding to mechanical loading. The life span of osteocytes is on the order of years; (76) therefore, cell numbers were unlikely to change within 1 week, and the osteocyte-associated gene expression at later time points almost certainly reflects higher transcriptional activity.

Spatial differences in cell-specific gene expression reflected the strain gradient along the cortex. Increased osteocyte (Sost) and decreased osteoclast (Ctsk) transcriptional activity suggested greater anabolism at the mid-diaphysis compared with the metaphyseal cortical shell. In this study, Sost expression was reduced with loading in the cortex, as recorded previously, (77) and also varied spatially along the cortex, a novel finding. The mid-diaphysis (highest strain) had greater Sost expression compared with lower strain tissue segments, suggesting enhanced osteocyte transcriptional activity due to lifelong loading. Osteocyte activity likely was influenced directly by strain magnitude; increasing strain led to more responding osteocytes as evaluated by intracellular calcium signaling. (78) In vivo murine tibial compression replicates physiologically relevant loading, with the highest tissue strains induced at the middiaphysis with normal daily activity. (13,19) Therefore, lifelong ambulation also could have influenced differences in cell populations across the cortex.

The relationship between the magnitude of the transcriptomic response and tissue-level bone formation warrants further investigation. Immediately after 2 weeks of in vivo tibial loading, cortical bone volume at the metaphyseal shell and mid-diaphysis was increased similarly, (13,79) a finding that does not mirror the unique transcriptomic responses reported here. However, 12 weeks after the cessation of loading, tissue-level increases at the mid-diaphysis were retained, whereas changes at the metaphyseal cortical shell were not. (80) In our results, a stronger load-induced anabolic transcriptional response at the mid-diaphysis may manifest in better long-term preservation of cortical bone compared with the metaphyseal cortical shell.

Several technical limitations affect the interpretation of our findings. The tissue within each segment is subject to both tension and compression at that location, and as analyzed, the

response to loading mode cannot be distinguished. Although the geometric differences between the tissue segments contributed directly to the gradient of strain magnitude, the heterogeneity in surface-area-to-volume ratios across each cortical location could contribute to biological differences as well. At present, the low number of cells obtained from the cortical segments precludes the analysis of transcriptomics for smaller tissue regions or individual cells. As single-cell RNA sequencing methods progress, the response of individual bone-resident cells should be associated with the applied strains. (81,82) In particular, emerging spatial transcriptomic methods could further localize the response to loading and elucidate potential differences in response to tensile and compressive strains. Our cell activity levels from sequencing data cannot distinguish between changes in cell activity and changes in cell numbers. Understanding that distinction would allow for development of therapeutics that specifically induce either cellular activation or cellular proliferation. (81) The biological pathways discussed in this study were identified using only transcriptomic data. (28) The protein- and tissue-level outcomes of the activation of these pathways await analysis at the proteomic level. Additionally, our detailed genes analysis was limited to 24 hours post-loading: extending to the other time points was beyond the scope of this study. Lastly, further investigation is required to translate the tissue strain-transcriptomic correlations to humans.

In conclusion, we found that cortical bone responds to mechanical loading as a function of strain magnitude across early and late time points. The importance of spatially varying gene expression is in contrast to most gene expression studies that examine the whole bone transcriptomic response to mechanical load. (15,16,83,84) Our group previously established tissue-specific differences in the transcriptomic response of cancellous and cortical bone to loading. (18) Based on these current data, gene expression in cortical bone should be distinguished by axial location or strain experienced. High strain magnitudes initiate larger, earlier anabolic responses in cortical bone. Conversely, low strain magnitudes have a slower anabolic response. This enhanced understanding of the role of strain in the in vivo cortical anabolic response will improve the ability to create targeted, effective therapeutics.

Disclosures

No author has any conflict of interest surrounding this work. MCHM has grants/grants pending from NIH, NSF, and DOD.

Acknowledgments

We thank Dr Qi Sun, Dr Adrian McNairn, Dr John Schimenti, Danielle Jorgenson, and the Cornell CARE staff.

Funding was provided by NSF grant no. 1636012, NSF GRFP (DGE-1650441), and GAANN P200A150273 J. The sponsors had no role in the writing or submission of the manuscript.

The experiments described in this manuscript were prospectively reviewed and approved by the Cornell University Institutional Animal Care and Use Committee.

Author Contributions

Carolyn Chlebek: Conceptualization; data curation; formal analysis; investigation; methodology; project administration; software; validation; visualization; writing – original draft; writing –

review and editing. Jacob A Moore: Data curation; formal analysis; software; validation; writing - review and editing. F. Patrick Ross: Conceptualization; formal analysis; funding acquisition; methodology; writing - review and editing. Mariolein C.H. van der Meulen: Conceptualization; funding acquisition; methodology; project administration; resources; supervision; writing review and editing.

Authors' roles: Concept and design: CC, FPR, and MCHM. Acquisition, analysis, and interpretation of data: CC, JAM, and MCHM. Drafting and critical revision of article: CC. JAM. FPR, and MCHM. Final approval of article: CC, JAM, FPR, and MCHM.

Peer Review

The peer review history for this article is available at https:// publons.com/publon/10.1002/jbmr.4686.

Data Availability Statement

Original data created for the study will be available in Gene Expression Omnibus upon publication.

References

- 1. Looker AC, Sarafrazi Isfahani N, Fan B, Shepherd JA. Trends in osteoporosis and low bone mass in older US adults, 2005-2006 through 2013-2014. Osteoporos Int. 2017;28(6):1979-1988.
- 2. Miller PD, Hattersley G, Riis BJ, et al. Effect of abaloparatide vs placebo on new vertebral fractures in postmenopausal women with osteoporosis: a randomized clinical trial. J Am Med Assoc. 2016;316(7): 722-733.
- 3. Neer RM, Arnaud CD, Zanchetta JR, et al. Effect of recombinant human parathyroid hormone (1-34) on fractures and bone mineral density in postmenopausal women with osteoporosis. N Engl J Med. 2001;344(19):1434-1441.
- 4. McClung MR, Grauer A, Boonen S, et al. Romosozumab in postmenopausal women with low bone mineral density. N Engl J Med. 2014; 370(5):412-420.
- 5. Cosman F, Crittenden DB, Adachi JD, et al. Romosozumab treatment in postmenopausal women with osteoporosis. N Engl J Med. 2016; 375(16):1532-1543.
- 6. Rubin MR, Bilezikian JP. The anabolic effects of parathyroid hormone therapy. Clin Geriatr Med. 2003;19(2):415-432.
- 7. Gennari L, Rotatori S, Bianciardi S, Nuti R, Merlotti D. Treatment needs and current options for postmenopausal osteoporosis. Expert Opin Pharmacother. 2016;17(8):1141-1152.
- 8. Jones H, Priest J, Hayes W, Tichenor C, Nagel D. Humeral hypertrophy in response to exercise. J Bone Jt Surg Am. 1977;59:204-208.
- 9. James MMS, Carroll S. Effects of different impact exercise modalities on bone mineral density in premenopausal women: a meta-analysis. J Bone Miner Metab. 2010;28(3):251-267.
- 10. Winters-Stone KM, Snow CM. Site-specific response of bone to exercise in premenopausal women. Bone. 2006;39(6):1203-1209.
- 11. Troy KL, Mancuso ME, Johnson JE, Wu Z, Schnitzer TJ, Butler TA. Bone adaptation in adult women is related to loading dose: a 12-month randomized controlled trial. J Bone Miner Res. 2020;35(7):1300-1312.
- 12. Main RP, Shefelbine SJ, Meakin LB, Silva MJ, van der Meulen MCH, Willie BM. Murine axial compression tibial loading model to study bone mechanobiology: implementing the model and reporting results. J Orthop Res. 2020;38(2):233-252.
- 13. Fritton JC, Myers ER, Wright TM, van der Meulen MCH. Loading induces site-specific increases in mineral content assessed by microcomputed tomography of the mouse tibia. Bone. 2005;36(6):1030-1038.

- 14. Main RP, Lynch ME, van der Meulen MCH, Load-induced changes in bone stiffness and cancellous and cortical bone mass following tibial compression diminish with age in female mice. J Exp Biol. 2014; 217(Pt 10):1775-1783.
- 15. Chermside-Scabbo CJ, Harris TL, Brodt MD, et al. Old mice have less transcriptional activation but similar periosteal cell proliferation compared to young-adult mice in response to in vivo mechanical loading. J Bone Miner Res. 2020;35(9):1751-1764.
- 16. Zaman G, Saxon LK, Sunters A, et al. Loading-related regulation of gene expression in bone in the contexts of estrogen deficiency, lack of estrogen receptor α and disuse. Bone. 2010;46(3):628-642.
- 17. Holquin N, Brodt MD, Silva MJ. Activation of Wnt signaling by mechanical loading is impaired in the bone of old mice. J Bone Miner Res. 2016;31(12):2215-2226.
- 18. Kelly NH, Schimenti JC, Ross FP, van der Meulen MCH. Transcriptional profiling of cortical versus cancellous bone from mechanicallyloaded murine tibiae reveals differential gene expression. Bone.
- 19. Patel TK, Brodt MD, Silva MJ. Experimental and finite element analysis of strains induced by axial tibial compression in young-adult and old female C57Bl/6 mice. J Biomech. 2014;47(2):451-457.
- 20. Razi H, Birkhold Al, Zaslansky P, et al. Skeletal maturity leads to a reduction in the strain magnitudes induced within the bone: a murine tibia study. Acta Biomater. 2015;13:301-310.
- 21. Birkhold Al, Razi H, Duda GN, Checa S, Willie BM. Tomography-based quantification of regional differences in cortical bone surface remodeling and mechano-response. Calcif Tissue Int. 2017;100(3):255-270.
- 22. Lynch ME, Main RP, Xu Q, et al. Tibial compression is anabolic in the adult mouse skeleton despite reduced responsiveness with aging. Bone. 2011:49(3):439-446.
- 23. Lynch ME, Main RP, Xu Q, et al. Cancellous bone adaptation to tibial compression is not sex dependent in growing mice. J Appl Physiol. 2010;109(3):685-691.
- 24. Kelly NH, Schimenti JC, Ross FP, van der Meulen MCH. A method for isolating high quality RNA from mouse cortical and cancellous bone. Bone. 2014;68:1-5.
- 25. Tandonnet S, Torres TT. Traditional versus 3' RNA-seg in a non-model species. Genomics Data. 2017;11:9-16.
- 26. Dobin A, Davis CA, Schlesinger F, et al. STAR: ultrafast universal RNAseg aligner. Bioinformatics. 2013;29(1):15-21.
- 27. Robinson MD, McCarthy DJ, Smyth GK. edgeR: a bioconductor package for differential expression analysis of digital gene expression data. Bioinformatics. 2010;26(1):139-140.
- 28. Subramanian A, Tamayo P, Mootha VK, et al. Gene set enrichment analysis: a knowledge-based approach for interpreting genomewide expression profiles. Proc Natl Acad Sci U S A. 2005;102(43): 15545-15550.
- 29. Ashburner M, Ball C, Black J, et al. Gene ontology: tool for the unification of biology. Nat Genet. 2000;25(1):25-29.
- 30. Carbon S, Douglass E, Good BM, et al. The gene ontology resource: enriching a GOld mine. Nucleic Acids Res. 2021;49(D1):D325-D334.
- 31. Jassal B, Matthews L, Viteri G, et al. The reactome pathway knowledgebase. Nucleic Acids Res. 2020;48(D1):D498-D503.
- 32. Komori T, Yagi H, Nomura S, et al. Targeted disruption of Cbfa1 results in a complete lack of bone formation owing to maturational arrest of osteoblasts. Cell. 1997;89(5):755-764.
- 33. Mark MP, Prince CW, Gay S, et al. A comparative immunocytochemical study on the subcellular distributions of 44 kDa bone phosphoprotein and bone γ -carboxyglutamic acid (Gla)-containing protein in osteoblasts. J Bone Miner Res. 1987;2(4):337-346.
- 34. Gerstenfeld LC, Chipman SD, Glowacki J, Lian JB. Expression of differentiated function by mineralizing cultures of chicken osteoblasts. Dev Biol. 1987;122(1):49-60.
- 35. Aubin JE. Advances in the osteoblast lineage. Biochem Cell Biol. 1998; 76(6):899-910.
- 36. Guo D, Keightley A, Guthrie J, Veno PA, Harris SE, Bonewald LF. Identification of osteocyte-selective proteins. Proteomics. 2010;10(20): 3688-3698.

- Westbroek I, De Rooij KE, Nijweide PJ. Osteocyte-specific monoclonal antibody MAb OB7.3 is directed against Phex protein. J Bone Miner Res. 2002;17(5):845-853.
- 38. Feng JQ, Huang H, Lu Y, et al. The dentin matrix protein 1 (Dmp1) is specifically expressed in mineralized, but not soft, tissues during development. J Dent Res. 2003;82(10):776-780.
- 39. Winkler DG, Sutherland MK, Geoghegan JC, et al. Osteocyte control of bone formation via sclerostin, a novel BMP antagonist. EMBO J. 2003;22(23):6267-6276.
- Nampei A, Hashimoto J, Hayashida K, et al. Matrix extracellular phosphoglycoprotein (MEPE) is highly expressed in osteocytes in human bone. J Bone Miner Metab. 2004;22(3):176-184.
- 41. Minkin C. Bone acid phosphatase: tartrate-resistant acid phosphatase as a marker of osteoclast function. Calcif Tissue Int. 1982;34(1): 285-290.
- 42. Drake FH, Dodds RA, James IE, et al. Cathepsin K, but not cathepsins B, L, or S, is abundantly expressed in human osteoclasts. J Biol Chem. 1996;271(21):12511-12516.
- Love MI, Huber W, Anders S. Moderated estimation of fold change and dispersion for RNA-seq data with DESeq2. Genome Biol. 2014; 15(12):1-21.
- 44. Shi Y, He G, Lee W-C, McKenzie JA, Silva MJ, Long F. Gli1 identifies osteogenic progenitors for bone formation and fracture repair. Nat Commun. 2017;8(1):2043.
- 45. Dowrey T, Schwager E, Duong J, Merkuri F, Zarate Y, Fish J. Satb2 regulates proliferation and nuclear integrity of pre-osteoblasts. Physiol Behav. 2017;176(5):139-148.
- Schmidt K, Schinke T, Haberland M, et al. The high mobility group transcription factor Sox8 is a negative regulator of osteoblast differentiation. J Cell Biol. 2005;168(6):899-910.
- 47. Zhang W, Liu P, Ling S, et al. Forkhead box P1 (Foxp1) in osteoblasts regulates bone mass accrual and adipose tissue energy metabolism. J Bone Miner Res. 2021;36(10):2017-2026.
- 48. Li Z, Wu G, Sher RB, et al. Choline kinase beta is required for normal endochondral bone formation. Biochim Biophys Acta. 2014;1840(7): 2112-2122.
- Canelon S, Wallace JM. Substrate strain mitigates effects of B-aminopropionitrile-induced reduction in enzymatic crosslinking. Calcif Tissue Int. 2019;105(6):660-669.
- 50. Zhao X, Deng P, Feng J, et al. Cysteine dioxygenase type 1 inhibits osteogenesis by regulating wnt signaling in primary mouse bone marrow stromal cells. Sci Rep. 2016;6:1-8.
- 51. Maurice SB, Bell T, Daniels T, et al. Tibial bone versican content decreases with zoledronate treatment in adult mice. Osteoporos Int. 2014;25(7):1975-1981.
- 52. Chan WL, Steiner M, Witkos T, et al. Impaired proteoglycan glycosylation, elevated TGF-β signaling, and abnormal osteoblast differentiation as the basis for bone fragility in a mouse model for gerodermia osteodysplastica. PLoS Genet. 2018;14(3):1-24.
- 53. van Dijk FS, Semler O, Etich J, et al. Interaction between KDELR2 and HSP47 as a key determinant in osteogenesis imperfecta caused by bi-allelic variants in KDELR2. Am J Hum Genet. 2020;107(5):989-999.
- Lv X, Gao F, Li TP, et al. Skeleton interoception regulates bone and fat metabolism through hypothalamic neuroendocrine NPY. eLife. 2021; 10:1-22.
- 55. Yan Y, Tang D, Chen M, et al. Axin2 controls bone remodeling through the β -catenin-BMP signaling pathway in adult mice. J Cell Sci. 2009;122(19):3566-3578.
- Fujiwara T, Ye S, Castro-Gomes T, et al. PLEKHM1/DEF8/RAB7 complex regulates lysosome positioning and bone homeostasis. JCI Insight. 2016;1(17):1-19.
- 57. Asagiri M, Takayanagi H. The molecular understanding of osteoclast differentiation. Bone. 2007;40(2):251-264.
- Fujita K, Iwasaki M, Ochi H, et al. Vitamin E decreases bone mass by stimulating osteoclast fusion. Nat Med. 2012;18(4): 589-594.

- Deng W, Wang L, Xiong Y, et al. The novel secretory protein CGREF1 inhibits the activation of AP-1 transcriptional activity and cell proliferation. Int J Biochem Cell Biol. 2015;65:32-39.
- Matsuoka K, Kohara Y, Naoe Y, et al. WAIF1 is a cell-surface CTHRC1 binding protein coupling bone resorption and formation. J Bone Miner Res. 2018;33(8):1500-1512.
- 61. Mattson AM, Begun DL, Molstad DHH, et al. Deficiency in the phosphatase PHLPP1 suppresses osteoclast-mediated bone resorption and enhances bone formation in mice. J Biol Chem. 2019;294(31): 11772-11784
- Inoue D, Kido S, Matsumoto T. Transcriptional induction of FosB/ΔFosB gene by mechanical stress in osteoblasts. J Biol Chem. 2004;279(48):49795-49803.
- Simonet WS, Lacey DL, Dunstan CR, et al. Osteoprotegerin: a novel secreted protein involved in the regulation of bone density. Cell. 1997;89(2):309-319.
- Ghosh M, Kelava T, Madunic IV, Kalajzic I, Shapiro LH. CD13 is a critical regulator of cell–cell fusion in osteoclastogenesis. Sci Rep. 2021; 11(1):1-14
- Maehata Y, Takamizawa S, Ozawa S, et al. Type III collagen is essential for growth acceleration of human osteoblastic cells by ascorbic acid 2-phosphate, a long-acting vitamin C derivative. Matrix Biol. 2007; 26(5):371-381.
- 66. Volk SW, Shah SR, Cohen AJ, et al. Type III collagen regulates osteoblastogenesis and the quantity of trabecular bone. Calcif Tissue Int. 2014;94(6):621-631.
- 67. Cheong VS, Roberts BC, Kadirkamanathan V, Dall'Ara E. Bone remodelling in the mouse tibia is spatio-temporally modulated by oestrogen deficiency and external mechanical loading: a combined in vivo/in silico study. Acta Biomater. 2020;116: 302-317.
- 68. Kimura H, Kwan KM, Zhang Z, et al. Cthrci is a positive regulator of osteoblastic bone formation. PLoS One. 2008;3(9):e3174.
- Takeshita S, Fumoto T, Matsuoka K, et al. Osteoclast-secreted CTHRC1 in the coupling of bone resorption to formation. J Clin Invest. 2013; 123(9):3914-3924.
- 70. Robinson JA, Chatterjee-Kishore M, Yaworsky PJ, et al. Wnt/ β -catenin signaling is a normal physiological response to mechanical loading in bone. J Biol Chem. 2006;281(42):31720-31728.
- Lemma S, Sboarina M, Porporato PE, et al. Energy metabolism in osteoclast formation and activity. Int J Biochem Cell Biol. 2016;79: 168-180.
- 72. Wei J, Shimazu J, Makinistoglu MP, et al. Glucose uptake and Runx2 synergize to orchestrate osteoblast differentiation and bone formation. Cell. 2015;161(7):1576-1591.
- 73. Galea GL, Meakin LB, Harris MA, et al. Old age and the associated impairment of bones' adaptation to loading are associated with transcriptomic changes in cellular metabolism, cell-matrix interactions and the cell cycle. Gene. 2017;599:36-52.
- 74. Huang J, Romero-Suarez S, Lara N, et al. Crosstalk between MLO-Y4 osteocytes and C2C12 muscle cells is mediated by the Wnt/ β -Catenin pathway. JBMR Plus. 2017;1(2):86-100.
- Manolagas SC. Birth and death of bone cells: basic regulatory mechanisms and implications for the pathogenesis and treatment of osteoporosis. Endocr Rev. 2000;21(2):115-137.
- Robling AG, Bonewald LF. The osteocyte: new insights. Annu Rev Physiol. 2020;82(1):485-506.
- Robling AG, Niziolek PJ, Baldridge LA, et al. Mechanical stimulation of bone in vivo reduces osteocyte expression of Sost/sclerostin. J Biol Chem. 2008;283(9):5866-5875.
- 78. Lewis KJ, Frikha-Benayed D, Louie J, et al. Osteocyte calcium signals encode strain magnitude and loading frequency in vivo. Proc Natl Acad Sci U S A. 2017;114(44):11775-11780.
- Galea GL, Hannuna S, Meakin LB, Delisser PJ, Lanyon LE, Price JS. Quantification of alterations in cortical bone geometry using site specificity software in mouse models of aging and the responses to ovariectomy and altered loading. Front Endocrinol. 2015;6: 1-11.

- 80. Javaheri B, Razi H, Gohin S, et al. Lasting organ-level bone mechanoadaptation is unrelated to local strain. Sci Adv. 2020; 6(10):eaax8301.
- 81. Greenblatt MB, Ono N, Ayturk UM, Debnath S, Lalani S. The unmixing problem: a guide to applying single-cell RNA sequencing to bone. J Bone Miner Res. 2019;34(7):1207-1219.
- 82. Ayturk U. RNA-seq in skeletal biology. Curr Osteoporos Rep. 2019; 17(4):178-185.
- 83. Morse A, Schindeler A, McDonald MM, Kneissel M, Kramer I, Little DG. Sclerostin antibody augments the anabolic bone formation response in a mouse model of mechanical tibial loading. J Bone Miner Res. 2018;33(3):486-498.
- 84. Armstrong VJ, Muzylak M, Sunters A, et al. Wnt/β-catenin signaling is a component of osteoblastic bone cell early responses to loadbearing and requires estrogen receptor α . J Biol Chem. 2007; 282(28):20715-20727.